

2015, 43 (115), 68–78
ISSN 1733-8670 (Printed)
ISSN 2392-0378 (Online)

Evaluation of near-collisions in the Tagus River Estuary using a marine traffic simulation model

Hao Rong, Angelo Teixeira, Carlos Guedes Soares

Universidade de Lisboa, Instituto Superior Técnico
Centre for Marine Technology and Ocean Engineering (CENTEC)
Avenida Rovisco Pais, 1049-001 Lisboa, Portugal
e-mails: {rong.hao; teixeira; c.guedes.soares}@centec.tecnico.ulisboa.pt

Key words: near-collisions, ship domain, marine traffic simulation, artificial potential field, AIS data, maritime safety

Abstract

This paper evaluates near ship-ship collision situations in the Tagus River Estuary using a simulation model of ship navigation in restricted waters. The simulation model consists of a ship collision avoidance model based on the Artificial Potential Field (APF) method, which has been improved to account for the lateral distribution of traffic along the route, the ship type and length and speed development of the ships along the trajectory. AIS data of ships entering and leaving the port of Lisbon are analysed to obtain the main characteristics of traffic parameters used as input for the traffic simulation model, such as: the routes of the vessels, speed distribution along the routes, traffic density and characteristics of the ships in each route, among others. First, the improved model of ship navigation and the Monte Carlo simulation technique are used to simulate the marine traffic in the Tagus River Estuary. Then, the concept of “ship domain” is used as collision criterion to determine the number of near collisions and the locations where they are most likely to occur. Finally, the simulation results are compared to the ones obtained from raw AIS data to assess the capability of the simulation model for marine traffic risk analysis.

Introduction

In the last decades several methods have been proposed for assessing ship collision risks (e.g. Montewka et al., 2010; Qu, Meng & Li, 2011; Li, Meng & Qu, 2012; Özbaş, 2013; Goerlandt & Montewka, 2015a, 2015b). The concept of “ship domain” proposed by Fujii and Tanaka (Fujii & Tanaka, 1971), defined as an area around the vessel which the navigator would like to keep free of other vessels for safety reasons, has been used as collision criterion in several collision assessment problems (e.g. Goodwin, 1975; Pietrzykowski, 2008). Ship domain models depend on the definition of the size of the domain, which may present significant variations (Wang et al., 2009).

Recent ship-ship collision probability estimation approaches are based on the assessment of the number of geometric collision candidates that typically relies on the calculation of a “collision diameter” (Fujii, Yamanouchi & Mizuki, 1970;

MacDuff, 1974; Pedersen, 1995) and on the definition of the causation probability (i.e. the probability that a pair of ships in a critical meeting situation (collision candidates) fail to avoid a collision).

Silveira et al. (Silveira, Teixeira & Guedes Soares, 2015) proposed a method to determine the number of collision candidates based on the available AIS messages. The method models pairs of ships as rectangles, using length and breadth information available in AIS messages. These rectangles are projected onto a line perpendicular to their relative velocity, (using course, heading and speed information from AIS) and the pair is considered a collision candidate if there is overlapping in the projections. A parametric study has been also performed by Silveira et al. (Silveira, Teixeira & Guedes Soares, 2015) to assess the contribution of important parameters of the proposed method on the collision candidates estimates.

Montewka et al. (Montewka et al., 2010) developed a method that replaces the geometric collision

diameter by a Minimum Distance To Collision (MDTC), a critical distance under which collision avoidance actions cannot prevent the collision from occurring. The value of this minimum distance depends on the crossing angle and on the ship type and is calculated based on a ship dynamics model. Based on the MDTC model the probability of maritime accidents was estimated (Montewka, Goerlandt & Kujala, 2012).

Hanninen and Kujala (Hanninen & Kujala, 2012) have analysed the role of human factors on ship collision probability based on a Bayesian network model. More recently, Montewka et al. (Montewka et al., 2014) and later Goerlandt and Montewka (Goerlandt & Montewka, 2015a) have proposed a framework for risk assessment for maritime transportation systems focusing on ship-ship collisions in the open sea involving RoRo/Passenger ships and oil spills from tankers. The risk framework was developed with the use of Bayesian Networks and utilises a set of analytical methods for the estimation of the risk model parameters.

Simulation models of ship navigation in congested waterways have been also adopted for collision assessment. Merrick et al. (Merrick et al., 2000) proposed marine traffic simulation model for risk analysis in coastal areas with input parameters derived from the analysis of AIS data. Goerlandt and Kujala (Goerlandt & Kujala, 2011) proposed a maritime traffic simulation model for ship collision probability assessment, which assumes that a ship does not take any sort of evasive action, corresponding to the assumption of blind navigation. Blokus-Roszkowska and Smolarek (Blokus-Roszkowska & Smolarek, 2012) presented an approach for modelling both spatial interactions and detailed succession dynamics in waterway crossings using a piecewise-deterministic Markov process.

Automatic ship navigation algorithms are also important tools for maritime traffic simulation. Xue (Xue et al., 2011) presented an effective and practical method for finding safe passage for ships in possible collision situations based on the artificial potential field (APF) method. The APF method has been used first by Khatib (Khatib, 1986) for robot path planning and later by Lee et al. (Lee, Kwon & Joh, 2004) who have introduced a fuzzy logic autonomous navigation algorithm based on the virtual field force (VFF), which is derived from the concept of potential field method.

Montewka et al. (Montewka et al., 2011) proposed a grounding probability assessment approach based on a gravity-like model in which the ship and

the navigational obstructions are perceived as interacting objects and their repulsion is modelled by a formulation inspired by the gravitational force. Xiao et al. (Xiao et al., 2013) described a microscopic nautical traffic simulation model that uses the artificial force field method as basis for the evasive and collision avoidance behaviour of ship interactions.

The APF method has been also used by Rong et al. (Rong, Teixeira & Guedes Soares, 2015) in a preliminary study to simulate the marine traffic in the Tagus River Estuary using a limited set of AIS data.

In the present paper the simulation model developed by Rong et al. (Rong, Teixeira & Guedes Soares, 2015) is improved by considering the lateral distribution of traffic along the route, the ship type, and length and speed development of the ships along the trajectory. The model is then used to simulate the maritime traffic in the Tagus River based on AIS data collected from 13th Jan. to 13th Feb. 2014 and to assess the near collisions using the concept of ship domain. The paper is organised as follows: section *AIS data analysis* presents the analysis of the AIS data of the Lisbon waterway; section *Artificial potential field method* introduces the potential field method applied to route finding for ships; section *Marine traffic simulation* presents the simulation results and a comparison with the AIS data; then section *Near-collisions evaluation* presents the results of the evaluation of the near collisions in the Tagus River Estuary from the simulated traffic and the observed AIS data.

AIS data analysis

The input parameters of the marine traffic simulation model are obtained from the analysis of AIS data collected during a period of one month (from 13th January to 13th February, 2014) in the area of the harbour of Lisbon. The sample of 5 515 118 AIS messages was first treated by removing stationary vessels and by correcting vessel speed errors based on the distance travelled between successive points and the elapsed time. Figure 1 shows the raw and cleaned AIS messages that are used in the present study.

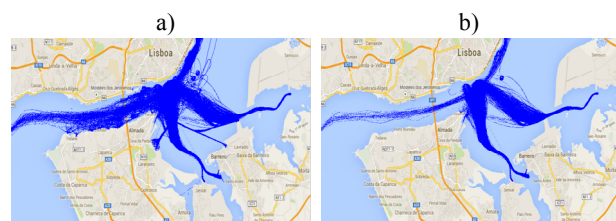


Figure 1. AIS position messages. a) raw data, b) cleaned data set

Main traffic routes in the Tagus River Estuary

Figure 1 exhibits several overlapping and well defined traffic trajectories. To identify main traffic routes (i.e. main traffic patterns), the AIS data are sorted by MMSI number and time to construct time-series of each vessel’s trajectory. A clustering algorithm is used to group similar trajectories into a main route based on the Hausdorff distance (e.g. Huttenlocher, Klanderma n & Rucklidge, 1993). The Hausdorff distance measures how far two subsets are from each other. In this context, the Hausdorff distance is adopted as an objective measure of each trajectory’s similarity. This technique is well-suited for clustering ship trajectories into different groups according to their similarity (Rong, Teixeira & Guedes Soares, 2015).

Figure 2 shows the marine traffic (Figure 1b) clustered into three main groups (i.e. three main traffic routes) (Figure 2 a–c), using an upper limit of 500 m for the Hausdorff distance. After clustering the AIS data, 3,168 ship trajectories have been grouped into 3 main routes. The number of trajectories in each group is presented in Table 1.

From Figure 2 it is clear that most vessels choose approximately the same path, but there is



Figure 2. Marine traffic flow: a) Cargo route, b) Barreiro Ferry route, c) Montijo Ferry route

Table 1. Distribution of trajectories in each route

Route	Total	Direction	
		North	South
Cargo route	74	41	33
Barreiro Ferry route	1214	572	642
Montijo Ferry route	1880	1010	870

also a deviation from the mean trajectory. This deviation is in some cases very large, for example at the north part of the Barreiro Route (Figure 2b), whereas at other locations the distribution over the waterway is relatively narrow. This indicates that the lateral distribution along the waterway needs to be investigated. This way, insights on the different traffic patterns can be obtained and used as input in the traffic simulation model.

At every 50 metres section along the main routes, the lateral traffic distribution is calculated from the available AIS data. Figure 3 shows an example of the lateral traffic distribution, derived from AIS data at a particular route section. On the x-axis, the zero value corresponds to the calculated mean of the trajectories. A positive value for x means that the vessel sails to the starboard side of the mean trajectory. A chi-square test showed that the lateral traffic distribution is well approximated by a normal distribution. The 95%-probability interval of the lateral traffic distribution is adopted to define boundaries of the waterway (see Figure 4). It should be noted that not all lateral distributions fit a normal distribution. However, it is convenient to consider that the deviation from the mean trajectory fits a normal distribution and this assumption leads to acceptable results for the purpose of this study.

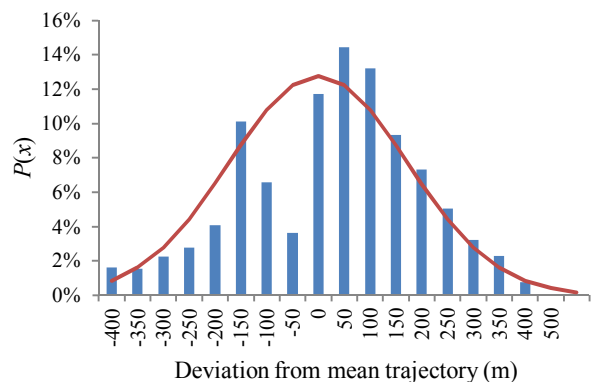


Figure 3. Lateral traffic distribution at a particular section of a main route (*p*-value = 0.74)

The above described procedure is repeated for every 50 metre section along the main routes. The cargo route is described by 493 sections and Barreiro and Montijo Ferry routes by 153 and 221 sections, respectively. The mean trajectory and the

boundaries of the cargo route are shown in Figure 4.



Figure 4. Mean trajectory and boundaries of the cargo route

Ship speed analysis

Typically, ships sail at their design speed in the open sea regardless of the destination, when environmental conditions permit. This implies that the ship speed distribution should be taken as strongly dependent on the ship type. In restricted waters, particularly in the river estuary, different ship types have different final destinations and therefore use different routes. The speed distributions of the considered ship types are shown in Figure 5.

The ship speed along the sections of the main traffic routes was also investigated. The speed distribution along the mean trajectory is derived from the average ship speed in each section. Figure 6 shows an interesting similarity between the mean speed evolutions along the three main traffic routes. Although the speed is definitely different, the shape of the two lines (Barreiro and Montijo routes) is very similar. One can observe a small reduction in speed at the entrance of the port in the cargo route mainly due to the fact that these vessels have to make a turn towards the port.

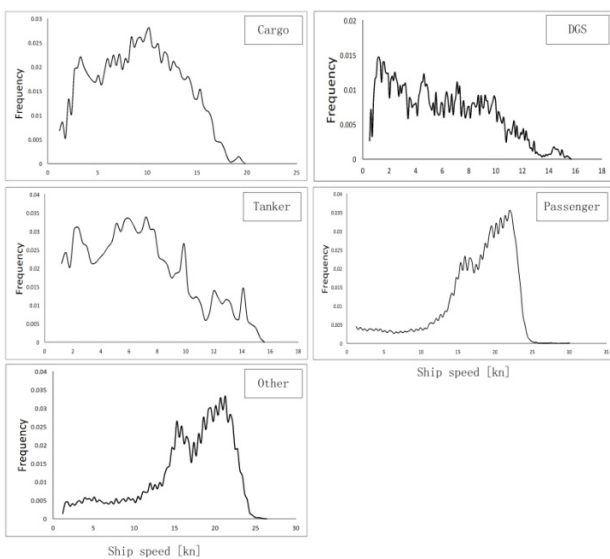


Figure 5. Ship speed distribution for each ship type

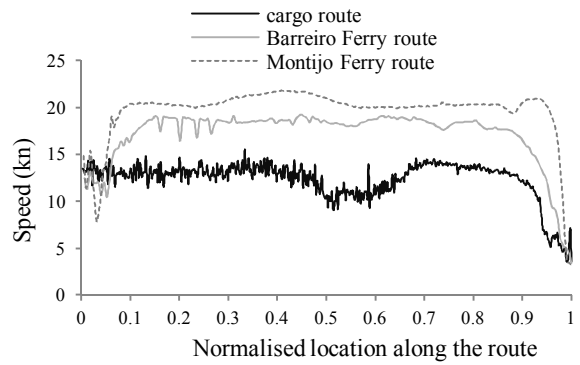


Figure 6. Mean speed evolution along the main traffic routes (location normalised by the route length)

Analysis of traffic flow in the harbour of Lisbon

Different routes are used by different ship types. For instance, the Barreiro Ferry route is mainly used by passenger ships, whereas traffic to and from the Sotagus Container Terminal consists mainly of cargo/container ships. Table 2 presents the ship type distribution in the study area.

Table 2. Distribution of ship types (%)

Route	Cargo route	Barreiro Ferry route	Montijo Ferry route
Cargo ship	76.2	7.7	9.9
Tanker	9.4	1.6	1.6
Passenger	2.7	89.3	87.9
DGS	7.2	0.2	0
other	4.5	1.2	0.6

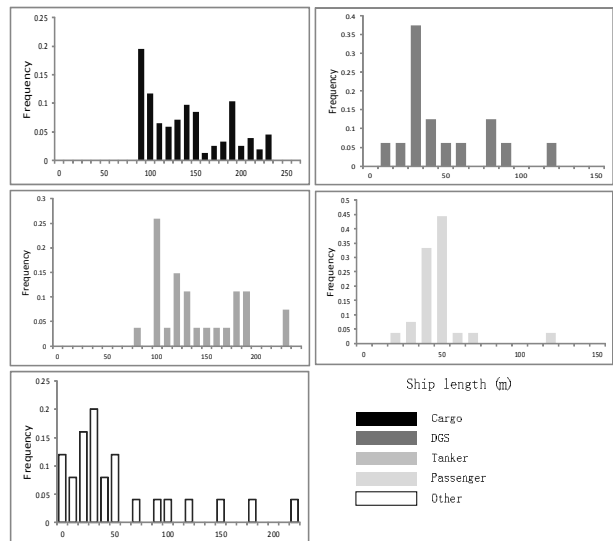


Figure 7. Ship length distribution for each ship type

The ship length distribution for each ship type was also obtained as this is an important input parameter of the simulation model that also affects the assessment of the collision risk. Figure 7 shows that the obtained ship length distribution for each ship type cannot be adequately described by any

theoretical distribution. Therefore, random sampling from the empirical distributions obtained from AIS data analysis is adopted in the simulation process.

Artificial potential field method

The artificial potential field (APF) (Khatib, 1986; Lee, Kwon & Joh, 2004) defines a potential energy field in the configuration space such that it has a minimum potential energy at the goal configuration. While the target is ideally at the minimum, all obstacles, or walls, are treated as high potential energy hills. In such a potential energy field, the ship is attracted to its goal position and repulsed from any obstacles (Figure 8).

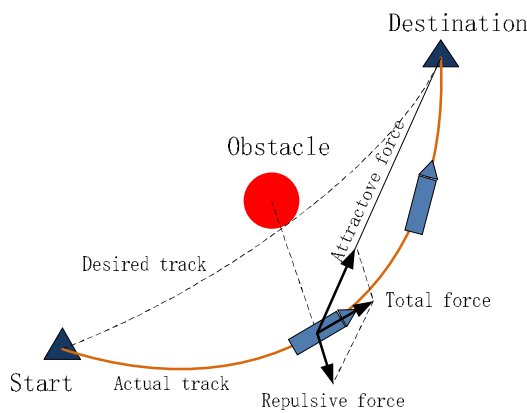


Figure 8. Potential field in ship's collision avoidance

The total potential energy at any point is the sum of the attractive potential due to the destination point and the repulsive potential due to the obstacle:

$$\bar{U}(\bar{p}) = \bar{U}_{att}(\bar{p}) + \bar{U}_{rep}(\bar{p}) \quad (1)$$

where $\bar{U}(\bar{p})$ is the total potential energy; $\bar{U}_{att}(\bar{p})$ is the potential energy due to attraction towards destination point; $\bar{U}_{rep}(\bar{p})$ is the potential energy due to repulsion of the obstacle; \bar{p} denotes a point on the water surface.

The ship is then subjected to a force which is derived from this potential field as follows:

$$\vec{F} = \vec{F}_{att} + \vec{F}_{rep} \quad (2)$$

where $\vec{F}_{att} = -\text{grad}(\bar{U}_{att}(\bar{p}))$, $\vec{F}_{rep} = -\text{grad}(\bar{U}_{rep}(\bar{p}))$.

Attractive potential energy

The attractive potential energy is a function of the relative distance between the ship and the destination point. The main characteristic of this function is that the value is high when they are far

apart, but then reduces gradually until it becomes null at the destination. The attractive potential energy function can, therefore, be written as follows:

$$\bar{U}_{att}(\bar{p}) = \alpha \|\bar{p}_d - \bar{p}(t)\|^m \quad (3)$$

where $\|\bar{p}_d - \bar{p}(t)\|$ is the Euclidean distance between the ship at time t and the destination position; α and m are the parameters of the model. A value of $m = 1.8$ has been adopted in the study, as proposed by Xue et al. (Xue et al., 2011).

Then the attractive force can be written as follows:

$$\begin{aligned} \vec{F}_{att}(\bar{p}) &= -\nabla \bar{U}_{att}(\bar{p}) = -\frac{\partial \bar{U}_{att}(\bar{p})}{\partial \bar{p}} = \\ &= m\alpha \|\bar{p}_d - \bar{p}(t)\|^{m-1} \end{aligned} \quad (4)$$

Repulsive potential energy

The repulsive potential energy $\bar{U}_{rep}(\bar{p})$ generated by the obstacle that keeps the ship in a safe distance can be written as follows:

$$\bar{U}_{rep}(\bar{p}) = \begin{cases} 0, & \text{when } \|\bar{p}_{tar_j}(t) - \bar{p}(t)\| - A > \rho_0 \\ \eta^* v_r^* \left[\frac{1}{\|\bar{p}_{tar_j} - \bar{p}(t)\| - A} - \frac{1}{\rho_0} \right], & \text{when } 0 < \|\bar{p}_{tar_j} - \bar{p}(t)\| - A < \rho_0 \\ \infty, & \text{when } \|\bar{p}_{tar_j} - \bar{p}(t)\| - A < 0 \end{cases} \quad (5)$$

where A and ρ_0 are the parameters of the model (Xue et al., 2011). Then the repulsive force can be written as follows:

$$\vec{F}_{rep}(\bar{p}) = \begin{cases} 0, & \text{when } \|\bar{p}_{tar_j}(t) - \bar{p}(t)\| - A > \rho_0 \\ -\frac{\partial \bar{U}_{rep}(\bar{p})}{\partial \bar{p}}, & \text{when } 0 < \|\bar{p}_{tar_j}(t) - \bar{p}(t)\| - A \leq \rho_0 \\ \infty, & \text{when } \|\bar{p}_{tar_j}(t) - \bar{p}(t)\| - A \leq 0 \end{cases} \quad (6)$$

The total potential and the total virtual force can be obtained from Eqs. (1) and (2). In the case where there are multiple obstacles, the repulsive force is given by:

$$\vec{F}_{rep}(\bar{p}) = \sum_{i=1}^{n_{obs}} (\vec{F}_{rep})_i \quad (7)$$

where n_{obs} is the number of obstacles and $(\bar{F}_{rep})_i$ denotes the repulsive force generated by the i -th obstacle.

Ship route modelling

One of the main tasks in applying the artificial potential field method for ship route finding concerns the representation of obstacles. In this case, for simplicity and flexibility, point primitives are used. The ship route can be represented by a series of point obstacles placed on the boundaries of the traffic route.

The algorithm used to find the main traffic routes was introduced above, and obstacle points are defined every 500 metres along the boundaries of the main routes. Figure 9 shows a particular route generated by the destination points and the discrete obstacle points producing the repulsive force that keep the ships in the traffic route. Figure 10 shows the simulation of one ship navigating in the cargo route (the red line is the ship trajectory). The ship’s speed was set to 10 kn, the starting point was at (0,0) and the influence range of the obstacles was set to 225 m. Figure 11 illustrates a simulation of a head-on encounter situation.

The simulations demonstrate that the developed algorithm is capable of automatically navigating

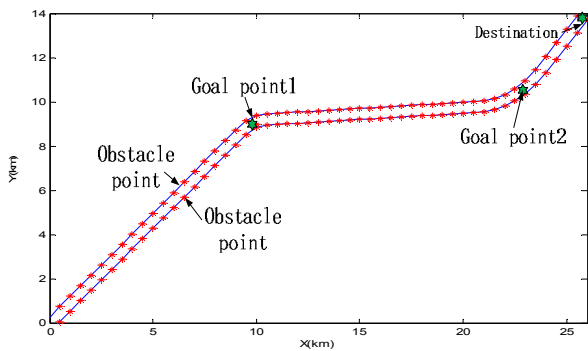


Figure 9. Route boundaries represented by a series of point obstacles

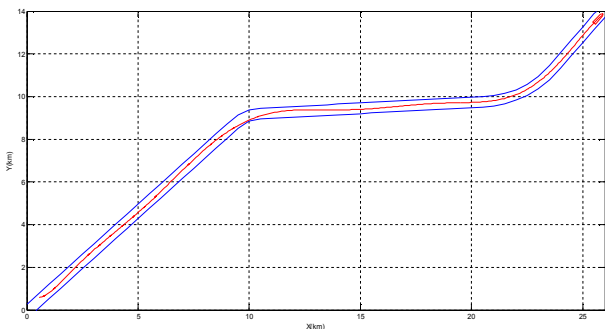


Figure 10. Simulation of the ship’s trajectory in the cargo route

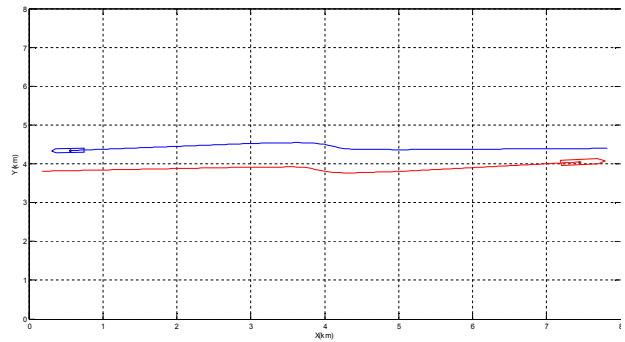


Figure 11. Simulation of a head-on situation

a ship through a waterway. It is true that the produced trajectory of the ship contains a few excessive manoeuvres, which a human pilot can judge to be bad practice. However, the main purpose of the current study is to investigate a method for implementing automatic simulation of ship navigation in the study area.

Marine traffic simulation

The traffic simulation consists of a micro-simulation process, which implies that the movements of each ship in the area (replicas of the traffic) are simulated in the time domain using the Monte Carlo simulations technique. The simulation model is route-based, where routes are characterised from AIS data and a statistical study of relevant traffic parameters and ship particulars on each route is first performed. The flow chart of the simulation model is shown in Figure 12. More details on the marine traffic simulation model can be found in Rong et al. (Rong, Teixeira & Guedes Soares, 2015).

Figure 13 shows the ship trajectories obtained based on 30 days of traffic simulation. In general, the results of the simulation of the ship trajectories show that the algorithm of the APF method is acceptable. Firstly, it is observed that the ships are navigating normally in the specific traffic lanes. Secondly, the ship trajectories from the simulation (shown in Figure 13) are similar to the ship trajectories from the AIS data (shown in Figure 1b). However, there are differences between the simulated ship trajectories with that of AIS data. Firstly, only the ships that navigate under the well-defined main routes (i.e. in the three main routes) are included in the simulation process. Some ships do not follow these patterns, navigating far away from the main traffic routes and their behaviour is unpredictable. Secondly, the ships that navigate towards other destinations (different from the ones considered) are not taken into account in the simulation model.

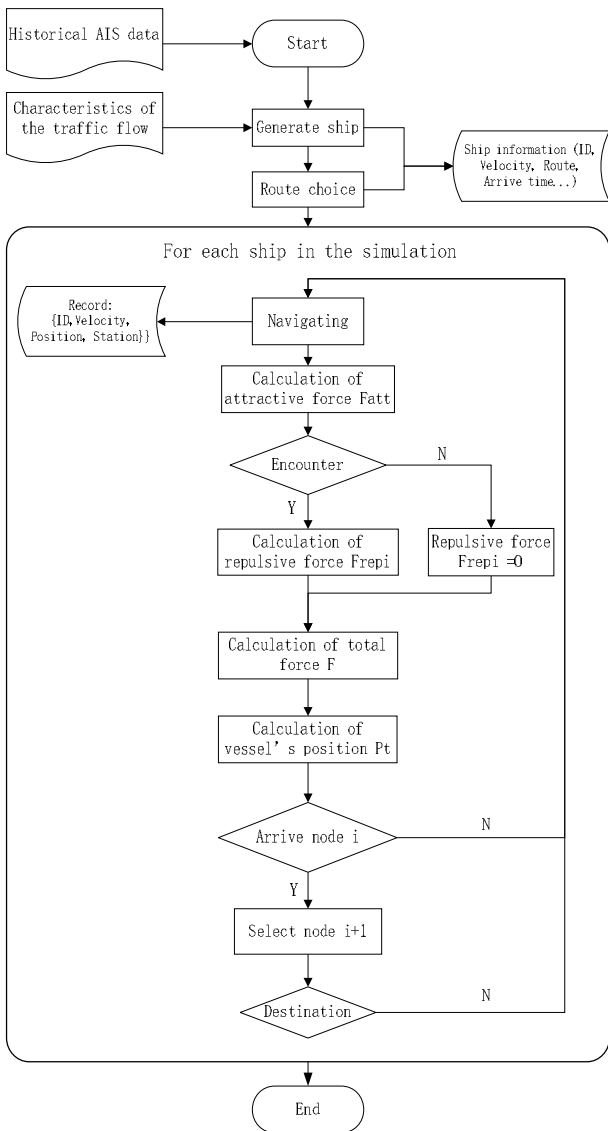


Figure 12. Flow chart of traffic simulation model

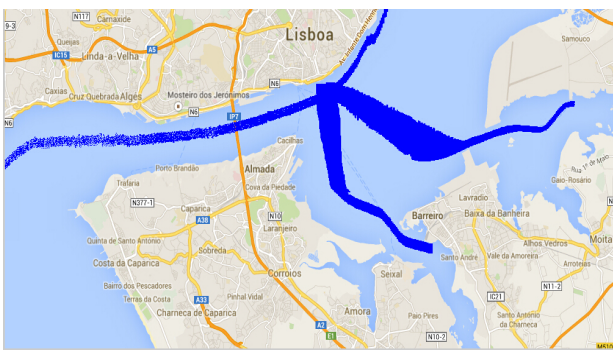


Figure 13. Simulation of ship trajectories in the three main routes

A comprehensive assessment of the simulation results is provided by Rong et al. (Rong, Teixeira & Guedes Soares, 2015) in terms of comparisons of important characteristics (such as mean velocity and acceleration and travel time) of the traffic simulated and observed from the AIS data. Rong

et al. (Rong, Teixeira & Guedes Soares, 2015) have considered that the ships did not change speed in the simulation, except when avoiding collisions and therefore the mean acceleration calculated from simulation was smaller than the one obtained from AIS data. In the present study the simulation model has been improved and now ships change speed along the traffic routes according to a speed profile derived from the AIS data, which has improved the simulation results.

In the current simulation model ships are generated (along with their physical attributes like length and ship type) and their trajectories are represented by a sequence of sub-trajectories, each of which is represented by an origin-destination pair. In the simulation, the strategy for updating the ships' velocities at each time step is based on their position along the route. Typically, the velocity increases at the beginning of the ship's trajectories and reduces to zero at the destination according to the speed profile shown in Figure 6.

Table 3 shows the average travel times for the various ships in the three main routes calculated with the improved simulation model. The table shows that the differences are now smaller than 3%. For some particular routes (Cargo and Barreiro Ferry routes) the simulation travel times are smaller than the actual ones, as some factors that may affect the travel time are not taken into consideration in the simulation model. A reasonable explanation is that ships in reality have more freedom to manoeuvre and to alter their speeds. Firstly, the ship speed is influenced by waterway geometry and secondly it is likely that ships have quite some interaction with other ships not accounted for in the simulation model as they were not sailing on the main routes considered. This leads to fewer speed changes in the simulation model than in reality and therefore ships in the simulation model are faster in general.

Table 3. Comparison between the actual travel time and the travel time derived from the simulation [in minutes]

Route	Travel time (AIS data)		Travel time (Simulation)		Difference (%)
	Mean (m)	Std. (m)	Mean (m)	Std. (m)	
Cargo route	47.497	3.141	46.317	2.157	-2.48
Barreiro Ferry route	28.355	5.183	27.583	4.057	-2.72
Montijo Ferry route	31.43	5.019	31.942	3.028	1.63

A comparison of the mean trajectories for each main route calculated by the simulation model and from AIS data was also performed. The results are expressed in terms of mean μ_{Δ} and standard deviation σ_{Δ} of the differences Δ_i between the mean

trajectories calculated by simulation and AIS data at each route section given by:

$$\begin{aligned}\mu_{\Delta} &= \frac{1}{n} \sum_{i=1}^n \Delta_i \\ \sigma_{\Delta} &= \sqrt{\frac{1}{n} \sum_{i=1}^n (\Delta_i - \mu)^2}\end{aligned}\quad (8)$$

where n is the number of sections of each route.

However, it should be noted that these differences are not independent from each other. For example, a high value for Δ_i makes it very likely also that Δ_{i-1} and Δ_{i+1} have a high value. Table 4 shows the mean and standard deviation obtained for the three different routes. A positive mean value indicates that the mean trajectory of simulation lies on the portside of the one derived from AIS data.

Table 4. Comparison of mean trajectories calculated by simulation and AIS data

Route	μ_{Δ}	σ_{Δ}
Cargo route	1.43	17.63
Barreiro Ferry route	4.16	4.97
Montijo Ferry route	8.12	12.48

Near-collisions evaluation

The near ship-ship collisions in the Tagus River Estuary are now analysed using the improved simulation model of ship navigation in restricted waters and raw AIS data directly. The approach adopted consists of identifying the near collisions using as collision criterion the concept of “ship domain”, first defined by Fujii and Tanaka (Fujii & Tanaka, 1971). This collision criterion is used to determine the number of near collisions and the locations where they are most likely to occur.

The concept of ship domain has been widely applied in navigational safety studies. A well-known definition of ship domain formulated by Goodwin (Goodwin, 1975) is described as “*the surrounding effective waters which the navigator of a ship wants to keep clear of other ships or fixed objects*”.

An analysis of near collisions in the Gulf of Finland was performed by Goerlandt et al. (Goerlandt et al., 2012), in which the Fujii ship domain was adopted as near collision criterion. Van Iperen (Iperen, 2012) combined ship domain and DCPA-TCPA methods to detect near misses in the North Sea. A distinction was made for head-on, crossing and overtaking near misses.

In this paper the ship domain proposed by Fujii and Tanaka (Fujii & Tanaka, 1971) is adopted, which consists of an ellipse centred at the position of the ship with semi-major a and semi-minor b

equal to 4 times and 1.6 times the ship length L , respectively, as shown in Figure 14a). As ship domain refers to waters that navigators want to keep clear of other ships, overlaps of ship domains or violation of a ship domain by another ship indicate higher likelihood of ship collisions.

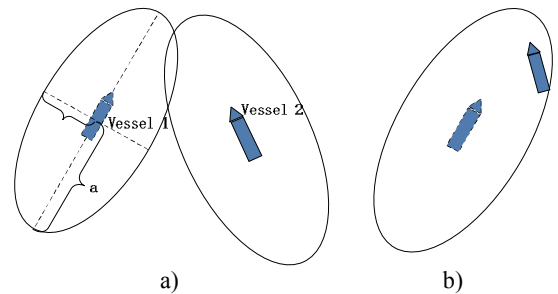


Figure 14. Fujii ship domain: a) overlap, b) violation

For calculating the near collisions, ship domains are defined for all ships based on position and COG data at all time steps T_i . If the domains overlap or are violated by another ship the encounters are defined as near collisions and the locations of these events are recorded.

Table 5 presents the number of near collisions corresponding to violations of ships domains with $a = 4L$, $a = 2L$ and $a = L$ derived from the traffic simulation, classified by the ship type involved. A total number of 289 ship domain violations were identified using an elliptical ship domain with $a = 4L$. The number of near collisions reduces when smaller ship domains are considered. In particular the domain violations reduce to almost half (128) when $a = 2L$ and further reduce to 68 for the smaller ship domain ($a = L$). The table also presents the number of ship domain overlaps that, as expected, is considerably higher than the number of ship domain violations.

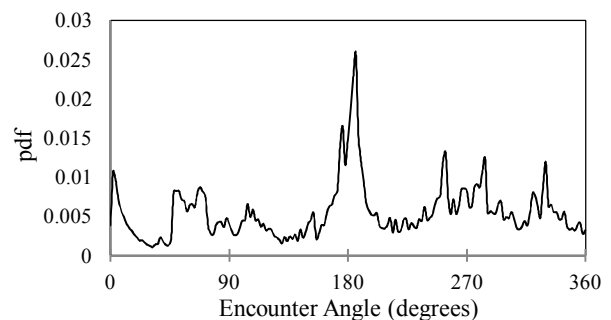


Figure 15. Distribution of encounter angle of ship domain violations

Figure 15 shows the distribution of the encounter angle of the ships involved in the near collision scenarios (corresponding to $a = L$), which demonstrates that the majority of the encounters correspond to head-on situations. It should be noted that

in all cases the ship domains are symmetric and do not take into account the International Regulations for Preventing Collisions at Sea (COLREGS). This directly affects the obtained number of ship domain violations especially in restricted waters.

For comparison purposes the ship domain violations were also evaluated based on the observed AIS data using the different ship domain sizes considered in Table 5. Table 6 shows that the ship domain violations obtained from the simulation model are underestimated. However, the overall relative proportion of violations classified by the ship type involved is similar. This is partly due to the fact that only the traffic on three main routes was considered in the simulation model and several crossings of these main routes have been neglected.

Table 5. Near collisions calculated from the traffic simulation model using different ship domain sizes

Ship type	Ship domain overlaps			Ship domain violations		
	$a=4L$	$a=2L$	$a=L$	$a=4L$	$a=2L$	$a=L$
Cargo-Cargo	39	15	2	16	3	0
Cargo-DGS	24	19	13	21	17	7
Cargo-Passenger	92	33	21	39	21	9
Cargo-Tanker	25	9	5	10	6	3
DGS-DGS	0	0	0	0	0	0
DGS-Passenger	2	1	1	1	1	0
DGS-Tanker	12	10	8	11	8	3
Passenger-Passenger	265	153	8	173	60	45
Passenger-Tanker	17	7	2	7	2	0
Tanker-Tanker	15	11	3	11	10	1
Total	491	258	162	289	128	68

Table 6. Ship domain violations calculated from raw AIS data

Ship type	Ship domain violations (Raw AIS data)		
	$a=4L$	$a=2L$	$a=L$
Cargo-Cargo	35	10	4
Cargo-DGS	26	20	13
Cargo-Passenger	85	36	17
Cargo-Tanker	24	8	5
DGS-DGS	2	0	0
DGS-Passenger	7	4	2
DGS-Tanker	12	11	9
Passenger-Passenger	223	116	69
Passenger-Tanker	17	3	1
Tanker-Tanker	16	10	4
Total	447	218	124

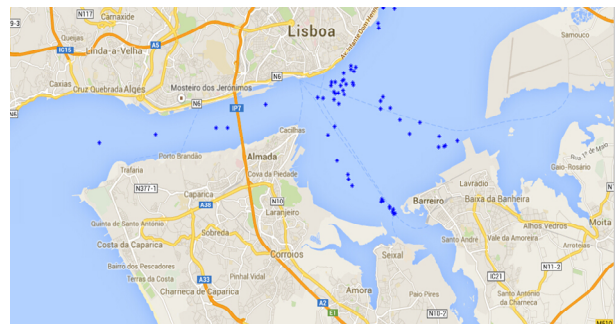
Table 7 shows the ship domain violations (ship domain with $a = 4L$ and L) divided according to the type of collision calculated using the simulation model and the AIS data. It is clear that the underestimation of the ship domain violations in crossing

encounters is the main contributor to the difference observed in the total number of near collisions calculated by the simulation and directly by the AIS data.

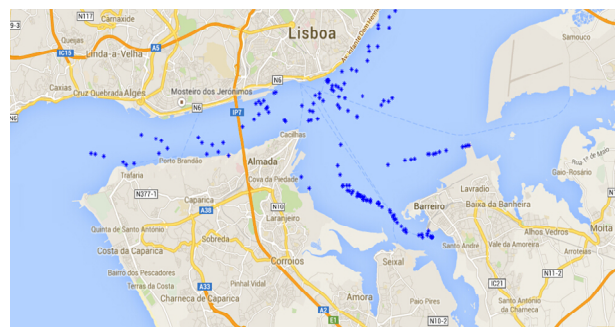
Table 7. Comparison of ship domain violations calculated from simulation and AIS data

Type of collision	Based on AIS data		Simulation model	
	$a=4L$	$a=L$	$a=4L$	$a=L$
Crossing	195	46	82	22
Head-on	133	31	125	38
Overtaking	182	59	111	31
Total	510	136	318	91

The locations of the ship domain violations obtained from the simulation model and identified from the AIS data are shown in Figure 16. It can be seen that the ship domain violations derived from the simulation are located only at the main traffic routes and several violations identified from AIS data are therefore not observed in the simulated traffic. The results indicate that the near collisions are very dependent on the geographic location. Due to its traffic density, the Barreiro Ferry route (Figure 2c) is the most probable location for ship near collisions. Another area in which the number of ship domain violations is high is the crossing between the cargo route (Figure 2b) and Barreiro Ferry route (Figure 2c).



a) collision candidates derived from simulation



b) collision candidates derived from AIS data

Figure 16. Locations of ship domain violations ($a = L$) derived from simulation and AIS data

The ship domain violations calculated from the simulation model are also very much dependent on the parameters of the APF method. In particular the influence range of repulsive field was set to 225 m in this study, which means if the distance between two ships is less than 225 m these two ships will be repulsed. As a result, the number of near collisions evaluated considering a ship domain with $a = L$ (the smallest ship domain) is considerably lower when compared with other ship domain sizes. However, the comparison of the results of the simulation with those of the AIS data provides important insights on how to calibrate the model parameters so that the simulation of traffic in restricted waters could be improved and used in collision risk assessments.

Conclusions

In this paper a marine traffic simulation model has been improved and used to evaluate the near-collisions in the Tagus river estuary. Compared with the previous simulation model used by the author, the current version takes into account the lateral distribution of traffic along the waterway, the speed distribution for different ship types and the speed development of the ships along the main routes. These new model parameters have improved considerably the results obtained from the traffic simulation. Moreover, other modifications on the APF method have been considered that also improved the prediction of the ships' trajectories in the presence of non-relevant obstacles.

The concept of "ship domain" was adopted as collision criterion to identify the near-collisions (ship domain overlaps or violations) both using the simulated traffic and raw AIS data. It was shown that the number of ship domain violations more than doubles (e.g. from 128 to 289) when the elliptical ship domain is increased from $a = 2L$ to $a = 4L$.

This pattern of results was obtained both when using the simulated traffic and the observed AIS data. However, the simulation model underestimates considerably the ship domain violations, as only the traffic on the main routes has been simulated and, therefore, several crossing encounters observed in the AIS data were not included in the simulation.

Moreover, the number of ship domain violations calculated by the simulation model depends on the parameters of the APF method. Therefore, the comparison of the ship violations derived from the simulated and observed traffic can be used to calibrate the model parameters so that simulation of traffic in restricted waters could be used when AIS

data are not available or to combine AIS data with simulated traffic of new routes.

Acknowledgments

This work has been financed by the Portuguese Foundation for Science and Technology under its annual funding to the Centre for Marine Technology and Ocean Engineering (CENTEC).

References

1. BLOKUS-ROSKOWSKA, A. & SMOLAREK, L. (2012) Collision Risk Estimation for Motorways of the Sea. *Reliability Theory and Practice*. 7. pp. 58–68.
2. FUJII, Y. & TANAKA, K. (1971) Traffic capacity. *Journal of Navigation*, 24 (4), 543–552.
3. FUJII, Y., YAMANOUCHI, H. & MIZUKI, N. (1970) On the fundamentals of marine traffic control. Part 1 probabilities of collision and evasive actions. *Electron. Navigation Res. Inst. Pap.* 2. pp. 1–16.
4. GOERLANDT, F. & KUJALA, P. (2011) Traffic simulation based ship collision probability modeling. *Reliability Engineering and System Safety*. 96 (1). pp. 91–107.
5. GOERLANDT, F. & MONTEWKA, J. (2015a) A Framework for Risk Analysis of Maritime Transportation Systems: A Case Study for Oil Spill from Tankers in a Ship-Ship Collision. *Safety Science*. 76. pp. 42–66.
6. GOERLANDT, F. & MONTEWKA, J. (2015b) Maritime Transportation Risk Analysis: Review and Analysis in Light of Some Foundational Issues. *Reliability Engineering & System Safety*. 138. pp. 115–34.
7. GOERLANDT, F., MONTEWKA, J., LAMMI, H. & KUJALA, P. (2012) Analysis of near Collisions in the Gulf of Finland. *In Advances in Safety, Reliability and Risk Management*, 2880–86. Troyes, France.
8. GOODWIN, E.M. (1975) A statistical study of ship domains. *Journal of Navigation*. 28(3). pp. 328–344.
9. HANNINEN, M. & KUJALA, P. (2012) Influences of variables on ship collision probability in Bayesian belief network model. *Reliability Engineering and System Safety*. 102. pp. 27–40.
10. HUTTENLOCHER, D.P., KLANDERMAN, G.A. & RUCKLIDGE, W.J. (1993) Comparing images using the Hausdorff distance. *Transactions on pattern analysis and machine intelligence*. 15 (9). pp. 850–863.
11. IPEREN, E. van (2012) Detection of Hazardous Encounters at the North Sea from AIS Data. *In Proceedings of International Workshop of Next Generation Nautical Traffic Models*. 1–12. Shanghai, China.
12. KHATIB, O. (1986) Real-time obstacle avoidance for manipulators and mobile robots. *Robotics Res.* 5(1). pp. 90–98.
13. LEE, S.M., KWON, K.Y. & JOH, J. (2004) A fuzzy autonomous navigation of marine vehicles satisfying COLREGS guidelines. *Control Autom.* 2(2). pp. 171–181.
14. LI, S., MENG, Q. & QU, X. (2012) An Overview of Maritime Waterway Quantitative Risk Assessment Models. *Risk Analysis*. 32 (3). pp. 496–512.
15. MACDUFF, T. (1974) The probability of vessel collisions. *Ocean Industry*. 9(9). pp. 144–148.
16. MERRICK, J.R.W., VAN DORP, J.R., HARRALD, J., MAZZUCHI, T., SPAHN, J. & GRABOWSKI, M. (2000) A systems approach approach to managing oil transportation risk in Prince William Sound. *System Engineering*. 3(3). pp. 128–142.

17. MONTEWKA, J., EHLERS, S., GOERLANDT, F., HINZ, T., TABRI, K. & KUJALA, P. (2014) A framework for risk assessment for maritime transportation systems – A case study for open sea collisions involving RoPax vessels. *Reliability Engineering and System Safety*. 124. pp. 142–157.
18. MONTEWKA, J., GOERLANDT, F. & KUJALA, P. (2012) Determination of collision criteria and causation factors appropriate to a model for estimating the probability of maritime accidents. *Ocean Engineering*. 40. pp. 50–61.
19. MONTEWKA, J., HINZ, T., KUJALA, P. & MATUSIAK, J. (2010) Probability modeling of vessel collision. *Reliability Engineering and System Safety*. 95(5). pp. 573–89.
20. MONTEWKA, J., KRATA, P., GOERLANDT, F., MAZAHERI, A. & KUJALA, P. (2011) Marine Traffic Risk Modelling – an Innovative Approach and a Case Study. *Proceedings of the Institution of Mechanical Engineers. Part O: Journal of Risk and Reliability*. 225 (3). pp. 307–22.
21. ÖZBAŞ, B. (2013) Safety Risk Analysis of Maritime Transportation: Review of the Literature. *Transportation Research Record: Journal of the Transportation Research Board*. 2326. pp. 32–38.
22. PEDERSEN, P.T. (1995) Collision and grounding Mechanics, The Danish Society of Naval Architects and Marine Engineers. pp. 125–57.
23. PIETRZYKOWSKI, Z. (2008) Ship's Fuzzy Domain – a Criterion for Navigational Safety in Narrow Fairways. *Journal of Navigation*. 62. pp. 499–514.
24. QU X.B., MENG, Q. & LI, S.Y. (2011) Ship collision risk assessment for the Singapore Strait. *Accident Analysis and Prevention*. 43 (6). pp. 2030–2036.
25. RONG H., TEIXEIRA A.P. & GUEDES SOARES, C. (2015) Simulation and analysis of maritime traffic in the Tagus River Estuary using AIS data. *Maritime Technology and Engineering*, Guedes Soares & Santos (Eds), Taylor & Francis Group. London. pp. 185–193.
26. SILVEIRA, P., TEIXEIRA, P.A. & GUEDES SOARES, C. (2015) Assessment of ship collision estimation methods using AIS data. *Maritime Technology and Engineering*, Guedes Soares & Santos (Eds), Taylor & Francis Group. London. pp. 195–204.
27. WANG, N., MENG, X., XU, Q., WANG, Z. (2009) A Unified Analytical Framework for Ship Domains. *Journal of Navigation*, 62, 643–655.
28. XIAO, F., LIGTERINGEN, H., GULIJK, C. van & ALE, B. (2013) Nautical Traffic Simulation with Multi-Agent System for Safety. *International Workshop on Next Generation Nautical Traffic Models 2013*. Delft, The Netherlands.
29. XUE, Y., CLELLAND, D., LEE, B.S. & HAN, D. (2011) Automatic simulation of ship navigation. *Ocean Engineering*. 38(17–18). pp. 2290–2305.
30. ZHANG, W., MONTEWKA, J. & GOERLANDT, F. (2015) Semi-Quantitative Method for Ship Collision Risk Assessment. *In Safety and Reliability: Methodology and Applications*. pp. 1563–72. Wroclaw, Poland.